Planetary transit reconstruction in the presence of stellar activity

Aude Alapini , Suzanne Aigrain UNIVERSITY OF EXETER

alapini@astro.ex.ac.uk

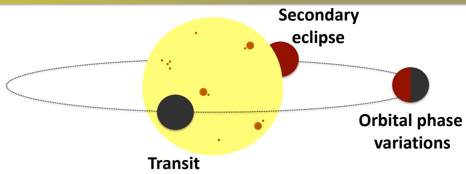

Abstract

Accurately characterising exoplanets is important to constrain planet formation and evolution models. In our quest for higher precision photometry to find Earth-size planets, we are increasingly challenged by stellar activity whose level in most stars is larger than the signal from a small planet, as shown in recent CoRoT results. Efficient methods to separate intrinsic stellar signal and small planetary signal, without altering the latter, are becoming essential.

We developed an Iterative Reconstruction Filter (IRF) which recovers the signals at the orbital period of the planet and improves the estimate of the planet parameters on average.

We apply the IRF to the CoRoT space photometry of the stars known to harbour planets in an attempt to refine the planet parameters and search for secondary eclipses and orbital phase variations.

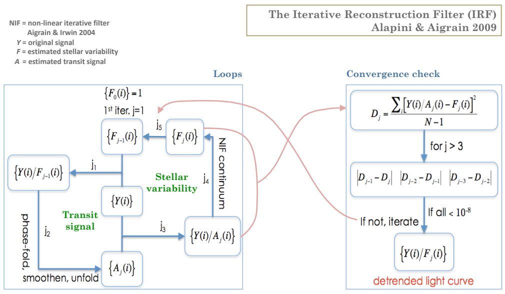

Iterative Reconstruction filter

The IRF removes stellar variability whilst altering the transit signal as little as possible by exploiting the knowledge of the planet period. It treats the light curve {Y(i)} as composed of the stellar variability {F(i)}, the transit signal {A(i)}, and some residuals {R(i)} such that: {Y(i)} = {F(i)} * {A(i)} + {R(i)}.

{F(i)} is taken as the Nonlinear Iterative Filter (NIF, Aigrain & Irwin 2004) continuum estimate of {Y(i)/A(i)} the light curve corrected from the transit signal. The IRF iterates to improve the estimate of {A(i)}, thus providing a better correction to the light curve and allowing a better estimate of {F(i)}, which is then fed into the next iteration to better estimate {A(i)}.

IRF applied to simulated CoRoT light curves

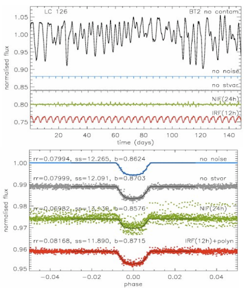

Figure 1 - Simulated CoRoT Blind Test 2 (BT2, Moutou et al. 2007) light curve (black) with Saturn-like transits barely visible due to stellar variability. NIF-filtered (green) and IRF-filtered (red) version of the same curve, original transit signal only (blue) and with instrumental noise (grey). Bottom: the NIF-filtered version shows an altered transit shape. The IRF recovers the shape of the transit (bottom, red), and preserves all signal at the period of the transit (top, red).

IRF applied to real CoRoT light curves: transit

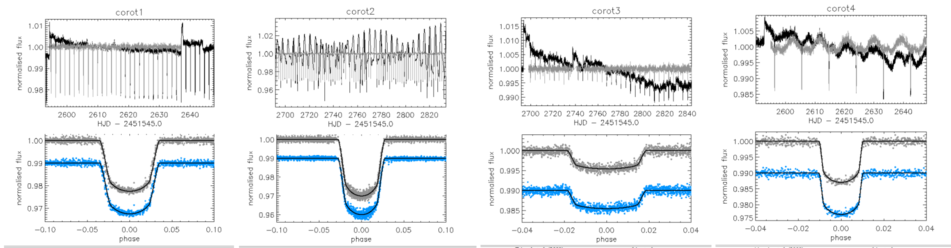

	Barge et al. (2008)	this study IRF 0.5d	this study IRF 0.25d
P [d]	1.5089557 ± 0.0000064	1.5091897 (fixed)	1.5091897 (fixed)
T_0 [d]	2454159.4532 ± 0.0001	2454159.45265 ± 0.00007	2454159.45265 ± 0.00007
$R_p/R_\star$	0.1388 ± 0.0021	0.1433 ± 0.0005	0.1432 ± 0.0006
$a/R_\star$	4.92 ± 0.08	4.56 ± 0.04	4.57 ± 0.04
i [°]	85.1 ± 0.5	83.1 ± 0.3	83.1 ± 0.3
u_a	0.42 ± 0.34	0.49 ± 0.02	0.49 ± 0.02
u_b	0.29 ± 0.34	0	0
e	0 (fixed)	0 (fixed)	0 (fixed)

	Alonso et al. (2008)	this study IRF 0.5d	this study IRF 0.25d
P [d]	1.7429964 ± 0.0000017	same (fixed)	same (fixed)
T_0[BJD]	2454237.53562 ± 0.00014	2454237.53535 ± 0.00003	2454237.53541 ± 0.00002
$R_p/R_\star$	0.1667 ± 0.0006	0.1622 ± 0.0004	0.1625 ± 0.0004
$a/R_\star$	6.70 ± 0.03	6.34 ± 0.03	6.30 ± 0.03
i [°]	87.8 ± 0.1	86.4 ± 0.1	86.3 ± 0.1
u_a	0.41 ± 0.03	0.491 ± 0.009	0.484 ± 0.007
u_b	0.06 ± 0.03	0	0
e	0 (fixed)	0 (fixed)	0 (fixed)

	Triaud et al. (2009) & Deleuil et al. (2008)	this study IRF 0.5d	this study IRF 0.25d
P [d]	$4.2567994^{+0.0000039}_{-0.0000031}$	same (fixed)	same (fixed)
T_0 [BJD]	$2454283.13388^{+0.00026}_{-0.00022}$	2454283.13946 ± 0.00024	2454283.13947 ± 0.00023
$R_p/R_\star$	$0.06632^{+0.00063}_{-0.00069}$	0.0665 ± 0.0007	0.0661 ± 0.0006
$a/R_\star$	$7.96^{+0.43}_{-0.35}$	7.03 ± 0.23	7.10 ± 0.23
i [°]	$86.1^{+0.7}_{-0.5}$	84.4 ± 0.4	84.6 ± 0.4
u_a	0.23 ± 0.09	0.47 ± 0.05	0.47 ± 0.05
u_b	0.33 ± 0.09	0	0
e	$0.008^{+0.005}_{-0.015}$	0 (fixed)	0 (fixed)
ω [°]	179 ± 170	0 (fixed)	0 (fixed)

	Aigrain et al. (2008) & Moutou et al. (2008)	this study IRF 0.5d	this study IRF 0.25d
P [d]	9.20205 ± 0.00037	same (fixed)	same (fixed)
T_0 [HJD]	2454141.36416 ± 0.00089	2454141.36433 ± 0.00027	2454141.36440 ± 0.00027
$R_p/R_\star$	$0.1047^{+0.0041}_{-0.0022}$	0.1053 ± 0.0009	0.1060 ± 0.0010
$a/R_\star$	$17.36^{+0.05}_{-0.25}$	16.8 ± 0.4	16.7 ± 0.4
i [°]	$90.000^{+0.000}_{-0.085}$	89.3 ± 0.4	89.2 ± 0.4
u_a	$0.44^{+0.16}_{-0.15}$	0.46 ± 0.03	0.47 ± 0.03
e	0.0 ± 0.1	0 (fixed)	0 (fixed)

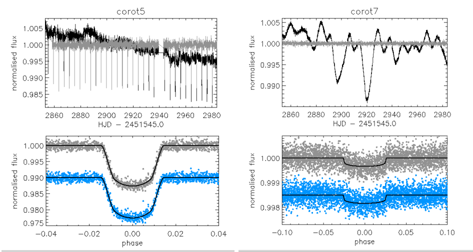

	Rauer et al. (2009)	this study IRF 0.5d	this study IRF 0.25d
P [d]	4.0378962 ± 0.0000019	same (fixed)	same (fixed)
T_0 [HJD]	2454400.19885 ± 0.0002	2454400.19844 ± 0.00016	2454400.19846 ± 0.00016
$R_p/R_\star$	$0.12087^{+0.00021}_{-0.00023}$	0.1120 ± 0.0009	0.1118 ± 0.0008
$a/R_\star$	8.97 ± 0.31	9.26 ± 0.18	9.27 ± 0.18
i [°]	$85.83^{+0.99}_{-1.38}$	85.5 ± 0.2	85.5 ± 0.2
u_a	0.308 fixed	0.62 ± 0.05	0.63 ± 0.05
u_b	0.308 fixed	0	0
e	$0.09^{+0.09}_{-0.04}$	0 (fixed)	0 (fixed)
ω [°]	-128^{+289}_{-48}	0 (fixed)	0 (fixed)

	Léger et al. (2009) & Queloz et al. (2009)	this study IRF 0.5d	this study IRF 0.25d
P [d]	0.853585 ± 0.000024	same (fixed)	same (fixed)
T_0 [HJD]	2454398.0767 ± 0.0015	2454398.07726 ± 0.00037	2454398.07716 ± 0.00031
$R_p/R_\star$	0.0187 ± 0.0003	0.0184 ± 0.0013	0.0182 ± 0.0012
$a/R_\star$	4.27 ± 0.20	4.13 ± 1.4	4.31 ± 1.2
i [°]	80.1 ± 0.3	79.3 ± 11.1	80.1 ± 8.8
u_a	0.40	same (fixed)	same (fixed)
u_b	0.20	same (fixed)	same (fixed)
e	0	0 (fixed)	0 (fixed)

Figure 2 - Pre-processed CoRoT planet host star light curves (black). IRF-filtered transit light curves with stellar variability estimated with IRF *timescale* of 0.5d (grey) and 0.25d (blue), and transit signal estimate with IRF *binsize* of $6*10^{-4}$ phase units. When the IRF-filtered transit signal has residual variability at the period of the transits, a 2nd order polynomial fits about the phase-folded transit is performed and divided from. The transit signal is fitted (black lines) using Mandel & Agol 2002 transit analytical formulation and a Levenberg-Marquardt algorithm to converge on the best model. The tables show the planet parameters derived from these best fits, compared to the published values. The uncertainties on the best fit parameters are evaluated by circularly permuting the residuals 100 times, re-evaluating the parameters each time, and taking the standard deviation of the values obtained for each parameter as the uncertainty on the parameter.

IRF applied to real CoRoT light curves: secondary eclipse

The search for a secondary eclipse in CoRoT-1b and CoRoT-2b IRF-filtered light curves is done using a sliding box varying both phase and duration. The resulting 2-D significance map ($S = \delta / \sigma * \sqrt{N}$) is shown below (white means high S). δ is the depth of the putative secondary derived as the difference between the median level in- and out-of-eclipse. σ is the local noise level per data point calculated as the standard deviation of the points outside the transits. N is the number points in-eclipse. For CoRoT-2b, a 2nd order polynomial function (black line, bottom right panel) is fitted about the phase-folded putative secondary and divided from, before estimating the in- and out-of-eclipse levels.

CoRoT-1b (see Alonso et al. 2009a)

IRF-filtering with *timescale* of 0.5d and *binsize* of 0.01 phase units

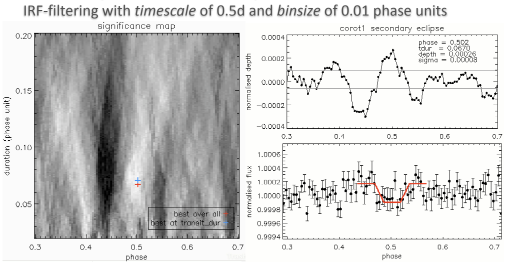

CoRoT-2b (see also Alonso et al. 2009b & Snellen et al. 2009b)

IRF-filtering with *timescale* of 0.25d and *binsize* of 0.005 phase units

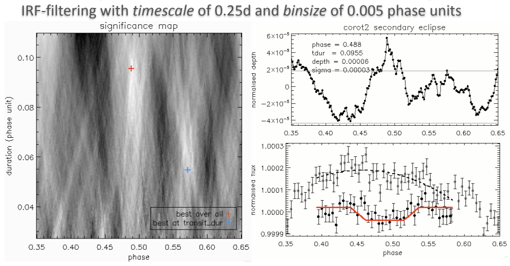

IRF applied to real CoRoT light curves: orbital phase variations

The light curve used here are the same as used for the secondary eclipse.

CoRoT-1b

The flux modulation at the transit period is comparable to that published in Snellen et al. 2009a.

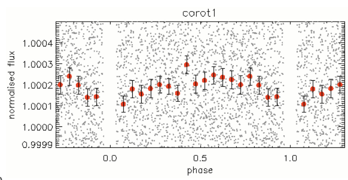

CoRoT-2b

The amplitude of the flux modulation at the transit period is too large to be of planetary origin only. It has a component of residual stellar activity at the orbital period of the planet.

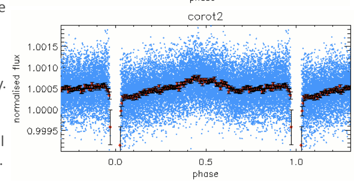

Conclusions

The IRF planet parameters are consistent with the published values implying that traditional variability filtering methods are not biasing our planet parameter estimates at the levels of stellar variability in these CoRoT light curves.

The IRF allows stellar variability filtering to lower time scales without affecting the transit shape, and in several cases appears to reduce the error bars on the derived planet parameters.

The IRF allows to search for secondary eclipses in the phase-folded light curve. However residual stellar variability and systematics imply only upper limits can be placed on orbital phase variations.

References:

Aigrain S., Irwin M., 2004, MNRAS, 350, 331
Aigrain S. et al., 2008, A&A, 488, L43
Alapini A., Aigrain S., 2009, MNRAS, 397, 159 1
Alonso R. et al., 2008, A&A, 482, L21
Alonso R. et al., 2009, A&A, 501, L23
Alonso R. et al., 2009, A&A accepted, arXiv:0907.1653
Barge P. et al., 2008, A&A, 482, L17
Deleuil M. et al. 2008, A&A, 491, 889
Léger A. et al., 2009, A&A accepted, arXiv:0908.0241
Mandel K., Agol E., 2002, ApJL, 580, L171
Moutou et al., 2007, ASPC, 366,127
Queloz D. et al. 2009, A&A accepted
Rauer H. et al. 2009, A&A accepted, arXiv:0909.3397
Snellen et al., 2009, Nature, 459, 543
Snellen et al., 2009, A&A submitted, arXiv:0909.4080
Triaud A. H. M. J. et al., 2009, A&A accepted, arXiv:0907.2956